Integration of Conductivity, Transparency, and Mechanical Strength into Highly Homogeneous Layer-by-Layer Composites of Single-Walled Carbon Nanotubes for Optoelectronics

Bong Sup Shim,[†] Zhiyong Tang,[†,||] Matthew P. Morabito,[†] Ashish Agarwal,[†] Haiping Hong,[§] and Nicholas A. Kotov*[,†,‡]

Department of Chemical Engineering, University of Michigan, Departments of Materials Science and Biomedical Engineering, University of Michigan, Ann Arbor, Michigan 48109, and South Dakota School of Mines and Technology, 501 East Saint Joseph Street, Rapid City, South Dakota 57701

Received February 14, 2007. Revised Manuscript Received July 25, 2007

Conductive organic and composite films represent the critical component of many areas of technology. This study demonstrates that highly conductive coatings can be made by layer-by-layer (LBL) assembly of single-walled carbon nanotubes (SWNTs). These films reveal electrical conductivities of 10^2 to $\sim 10^3$ S/m at room temperature without doping with nanotube loading as low as ~10%. This is indicative of efficient utilization of SWNT in percolation pathways. Low SWNT loading also makes the coatings quite transparent with transmission as high as 97% for visible light. Thicker delaminated LBL films displayed conductivities of 4.15×10^4 S/m. The free-standing films were highly flexible and possessed 160 MPa of tensile strength, which makes them the strongest organic conductor. The high strength and conductivities are attributed to the unique homogeneity of the LBL assembled composites, which opens the way to future optimization of electrical, mechanical, and optical properties and to fit the needs of specific applications, which may be exemplified by transparent flexible electronics, light emitting diodes, smart windows, solar cells, sensors, structural materials, and biomedical devices.

Introduction

An individual single-walled carbon nanotube (SWNT) possesses unique electrical, optical, and mechanical properties attributed to sp^2-hybridized bonds in the perfect graphene roll. The tensile strength and Young's modulus of a SWNT are estimated to be 37 and 640 GPa, respectively,[1,2] and the electrical conductivities of their metallic ropes are 1 to ~3 $\times 10^6$ S/m.[3] The grand challenge of today's material science is the transfer of unique properties observed in the nanoscale structures into the bulk materials and macroscale technological elements. It can be achieved fairly easily with the luminescence of nanoparticles,[4] but for other properties such as mechanical strength, electrical, and thermal properties. This task brings about much more difficult challenges of processing of nanoscale building blocks (rods, tubes, wires, spheres, triangles, etc.) into macroscale materials. As such, a large variety of processing methods of various degrees of complexity were developed for SWNTs.[5−7] As a rule of thumb, the most essential technological properties require the uniformity of distribution of nanoparticles in the connecting matrix.

One of the most reliable nanofabrication methods of reaching a monomolecular level homogeneity from virtually any nanoscale building block is the sequential deposition of nanometer thick layers of polymer and nanocolloids, known as the layer-by-layer (LBL) assembly, which also makes it possible to achieve nanocomposites with exceptional homogeneity by overcoming self-aggregation of both single-walled[8] and multiwalled[9] nanotubes. In each adsorption layer, the nanotubes in a dilute solution are directly immobilized into a solid with sufficient anchoring interactions on the previous layer so that no matrix−nanotube phase separation takes place. The same is likely to be applied to other nanocolloids with different geometries other than axial,[10] such as planar in the case of clay,[11] or metallic triangles,[12] and spherical particles.[4] LBL assembly affords preparation of

* Corresponding author. E-mail: kotov@umich.edu.
[†] Department of Chemical Engineering, University of Michigan.
[‡] Departments of Materials Science and Biomedical Engineering, University of Michigan.
[§] South Dakota School of Mines and Technology.
[||] Present address: National Center for Nanoscience and Technology, Beijing 100080, China.

(1) Baughman, R. H.; Zakhidov, A. A.; de Heer, W. A. *Science* **2002**, *297* (5582), 787−792.
(2) Yu, M. F.; Files, B. S.; Arepalli, S.; Ruoff, R. S. *Phys. Rev. Lett.* **2000**, *84* (24), 5552−5555.
(3) Thess, A.; Lee, R.; Nikolaev, P.; Dai, H.; Petit, P.; Robert, J.; Xu, C.; Lee, Y. H.; Kim, S. G. *Science* **1996**, *273* (5274), 483−487.
(4) Mamedov, A. A.; Belov, A.; Giersig, M.; Mamedova, N. N.; Kotov, N. A. *J. Am. Chem. Soc.* **2001**, *123* (31), 7738−7739.
(5) Niyogi, S.; Hamon, M. A.; Hu, H.; Zhao, B.; Bhowmik, P.; Sen, R.; Itkis, M. E.; Haddon, R. C. *Acc. Chem. Res.* **2002**, *35* (12), 1105−1113.
(6) Banerjee, S.; Hemraj-Benny, T.; Wong, S. S. *Adv. Mater.* **2005**, *17* (1), 17−29.
(7) Lin, Y.; Taylor, S.; Li, H.; Fernando, K. A. S.; Qu, L.; Wang, W.; Gu, L.; Zhou, B.; Sun, Y. P. *J. Mater. Chem.* **2004**, *14* (4), 527−541.
(8) Mamedov, A. A.; Kotov, N. A.; Prato, M.; Guldi, D. M.; Wicksted, J. P.; Hirsch, A. *Nat. Mater.* **2002**, *1* (3), 190−194.
(9) Olek, M.; Ostrander, J.; Jurga, S.; Moehwald, H.; Kotov, N.; Kempa, K.; Giersig, M. *Nano Lett.* **2004**, *4* (10), 1889−1895.
(10) Wang, Y.; Tang, Z.; Podsiadlo, P.; Elkasabi, Y.; Lahann, J.; Kotov, N. A. *Adv. Mater.* **2006**, *18* (4), 518−522.

10.1021/cm070442a CCC: $37.00
Published on Web 10/10/2007

solid film and membranes up to a few tens of micrometers in thickness.[8,13] This is sufficient to investigate the bulk properties of the prepared composites. Also, this is the preferred starting point for a variety of applications, such as biomedical,[14,15] optoelectronic and radioelectronic devices, gas separation membranes,[16] laminated structural composites, and sensors.[17]

In the past, we studied the strength of LBL nanocomposites and gained substantial improvement over similar materials.[8] The conjecture that high uniformity of the SWNT distribution in the matrix is essential not only for the mechanical properties, but also for charge transport, served as an inspiration to this work. Recently, Kovtyukhova and Mallouk reported that LBL films of partially oxidized SWNT and conductive polymer (polyaniline (PAN)) showed electrical conductivities with a maximum of 5×10^2 S/m.[18] However, oxidation partially destroys the conjugation of aromatic rings of SWNTs with apparent detriment for charge transfer. In this work, we demonstrate that LBL films can be obtained from pristine SWNTs which result in more than an order of magnitude improvement of the conductivity. They are also mechanically strong and flexible; their tensile strength significantly exceeds that of typical organic conductors and is comparable or on par with the tensile strength of materials containing 100% SWNTs.[19−21] LBL assembly affords one the ability to control the contents of SWNTs in the film, the overall thickness, and distance between the individual nanotubes. Consequently, one can make films not only conductive, but also transparent, which has significant technological value.[22] Importantly, even a few multilayers were found to be sufficient to create a fully conductive coating with transparency as high as 97%. This is a winning combination of parameters for optoelectronics and energy harvesting. As such, such coatings can potentially replace indium tin oxide (ITO) substrates in solar cells; ITO becomes quite expensive due to a shortage of indium. Additionally, the major outcome of the paper is more complete functional utilization of the unique properties of nanoscale building blocks with axial geometry.

Results and Discussion

Film Preparation and Structural Characteristics. Fabrication of a homogeneous SWNT−polymer composite must start from the preparation of a well-dispersed SWNT solution. The quality of nanocolloids, as it relates to the degree of dispersion, can be preserved in the resulting material because micrometer-scale reorganization of the LBL multilayers is prevented due to the restricted mobility of the long SWNT fibers.[8] This is also applicable to other nanocolloids assembled by the same techniques. The complete exfoliation can be achieved by wrapping the nanotubes with charged aromatic polymers such as poly(sodium 4-styrene-sulfonate) (PSS) owing to $\pi-\pi$ and hydrophobic interactions.[23−25] This also avoids the oxidation step for SWNT necessary for solubilization in older schemes[8,18,26] to prevent deterioration of electrical properties of the individual nanotubes. At the same time it introduces a dielectric shell around the nanotubes. The bottleneck in the conductivity in both wrapped and oxidized nanotubes may not be the defects in the individual nanotubes but rather their spatial distribution and the probability of charge hopping from one SWNT to another.[27−29] A proper balance between the method of dispersion and electrical conductivity is still to be found. It will likely require computer modeling of charge transport in the percolation network of the nanotubes and establishing the charge tunneling parameters for SWNT−SWNT contacts.

We hypothesized that better transport properties are more likely to be found when nanotubes are intact and took advantage of the methods of tuning of the molecular structure of the LBL stacks available to us. So, the LBL assembly was realized with a stable 0.1% SWNT dispersion in 0.2% PSS as component no. 1 and a 1% solution of poly(vinyl alcohol) (PVA) as component no. 2. The substrates were alternatively dipped in these solutions, producing stacks with cumulative structures $[PVA/(SWNT + PSS)]_n$, where n is the number of deposition cycles. Interestingly, the SWNT−PSS dispersion is attracted to PVA strongly enough to form an LBL assembly, whereas PVA is neutral. The alternate adsorption occurs predominantly due to hydrogen bonds, van der Waals, and to a lesser extent electrostatic interactions. The importance of the perceived "weak" interactions in the LBL adsorption was previously demonstrated theoretically.[30]

(11) Tang, Z.; Kotov, N. A.; Magonov, S.; Ozturk, B. *Nat. Mater.* **2003**, *2* (6), 413−418.
(12) Malikova, N.; Pastoriza-Santos, I.; Schierhorn, M.; Kotov, N. A.; Liz-Marzan, L. M. *Langmuir* **2002**, *18* (9), 3694−3697.
(13) Rouse, J. H.; Lillehei, P. T.; Sanderson, J.; Siochi, E. J. *Chem. Mater.* **2004**, *16* (20), 3904−3910.
(14) Gheith, M. K.; Sinani, V. A.; Wicksted, J. P.; Matts, R. L.; Kotov, N. A. *Adv. Mater. (Weinheim, Ger.)* **2005**, *17* (22), 2663−2670.
(15) Gheith, M. K.; Pappas, T. C.; Liopo, A. V.; Sinani, V. A.; Shim, B. S.; Motamedi, M.; Wicksted, J. P.; Kotov, N. A. *Adv. Mater. (Weinheim, Ger.)* **2006**, *18* (22), 2975−2979.
(16) Kotov, N. A.; Magonov, S.; Tropsha, E. *Chem. Mater.* **1998**, *10* (3), 886−895.
(17) Loh, K. J.; Lynch, J. P.; Kotov, N. A. *Proc. SPIEsInt. Soc. Opt. Eng.* **2006**, *6174*, 61741Z-1−61741Z/12.
(18) Kovtyukhova, N. I.; Mallouk, T. E. *J. Phys. Chem. B* **2005**, *109* (7), 2540−2545.
(19) Ericson, L. M.; Fan, H.; Peng, H.; Davis, V. A.; Zhou, W.; Sulpizio, J.; Wang, Y.; Booker, R.; Vavro, J.; Guthy, C.; Parra-Vasquez, A. N.; Kim, M. J.; Ramesh, S.; Saini, R. K.; Kittrell, C.; Lavin, G.; Schmidt, H.; Adams, W. W.; Billups, W. E.; Pasquali, M.; Hwang, W. F.; Hauge, R. H.; Fischer, J. E.; Smalley, R. E. *Science* **2004**, *305* (5689), 1447−1450.
(20) Zhang, X.; Sreekumar, T. V.; Liu, T.; Kumar, S. *J. Phys. Chem. B* **2004**, *108* (42), 16435−16440.
(21) Kozlov, M. E.; Capps, R. C.; Sampson, W. M.; Ebron, V. H.; Ferraris, J. P.; Baughman, R. H. *Adv. Mater.* **2005**, *17* (5), 614−617.
(22) Unalan, H. E.; Fanchini, G.; Kanwal, A.; Du Pasquier, A.; Chhowalla, M. *Nano Lett.* **2006**, *6* (4), 677−682.
(23) O'Connell, M. J.; Boul, P.; Ericson, L. M.; Huffman, C.; Wang, Y.; Haroz, E.; Kuper, C.; Tour, J.; Ausman, K. D.; Smalley, R. E. *Chem. Phys. Lett.* **2001**, *342* (3, 4), 265−271.
(24) Kim, B.; Park, H.; Sigmund, W. M. *Langmuir* **2003**, *19* (6), 2525−2527.
(25) Sinani, V. A.; Gheith, M. K.; Yaroslavov, A. A.; Rakhnyanskaya, A. A.; Sun, K.; Mamedov, A. A.; Wicksted, J. P.; Kotov, N. A. *J. Am. Chem. Soc.* **2005**, *127* (10), 3463−3472.
(26) Kovtyukhova, N. I.; Mallouk, T. E. *Adv. Mater.* **2005**, *17* (2), 187−192.
(27) Vigolo, B.; Coulon, C.; Maugey, M.; Zakri, C.; Poulin, P. *Science* **2005**, *309* (5736), 920−923.
(28) Grunlan, J. C.; Mehrabi, A. R.; Bannon, M. V.; Bahr, J. L. *Adv. Mater.* **2004**, *16* (2), 150−153.
(29) Fuhrer, M. S.; Nygard, J.; Shih, L.; Forero, M.; Yoon, Y. G.; Mazzoni, M. S. C.; Choi, H. J.; Ihm, J.; Louie, S. G.; Zettl, A.; McEuen, P. L. *Science* **2000**, *288* (5465), 494−497.
(30) Kotov, N. A. *Nanostruct. Mater.* **1999**, *12*, 789−796.

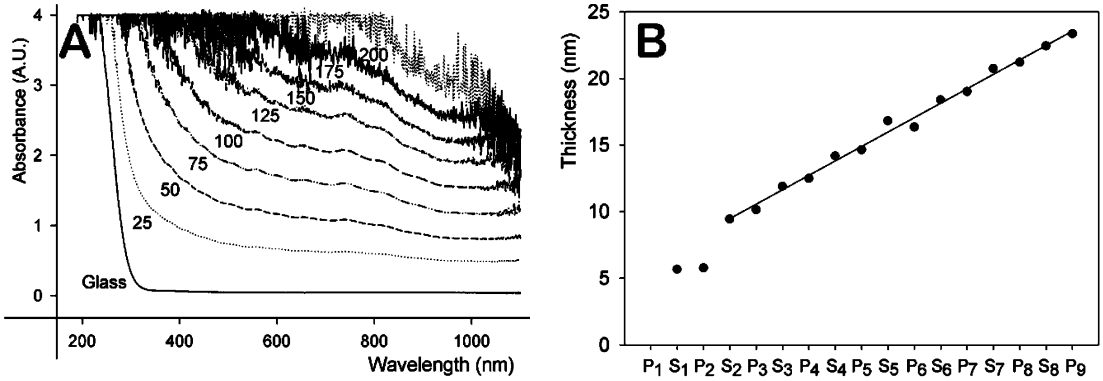

Figure 1. (A) UV−vis absorbance spectra measured every 25th bilayer of $[PVA/(SWNT + PSS)]_n$ LBL assemblies. The multilayers were formed on both sides of a glass substrate. The numbers by the curve indicate *n*. (B) Dependence of the thickness of the $[PVA/(SWNT + PSS)]_n$ film on the number of deposition cycles. PVA (P_n) and SWNT (S_n) layers with the same *n* correspond to one deposition cycle. Thickness changes were measured by ellipsometry as the LBL film was formed on a Si wafer. The displayed thicknesses of each component layer is an average of three ellipsometric measurements.

PVA was chosen over a positively charged polyelectrolyte because this polymer has specific affinity to nanotubes producing high-strength materials.[31−33] Regardless of the absence of a traditional ± attractive electrostatic component in the interactions of PVA and PSS or SWNTs, UV−vis monitoring of the dependence on *n* demonstrated a linear increment in $[PVA/SWNT + PSS]_n$ thickness and light absorbance (Figure 1, parts A and B).

As is often the case with LBL films, there is an initial lag period in the accumulation of LBL multilayers on the substrate manifesting in smaller thickness increments (Figure 1B). After $n = 2$, the ellipsometry readings follow a straight line; the average thickness increments of SWNT layers and PVA layers in initial LBL assembly stages were calculated to 1.77 and 0.47 nm, respectively. Looking at the UV−vis spectra, one should also point out the prominent van Hove singularity peaks. Their presence is a strong evidence of homogeneous dispersion of exfoliated SWNTs in the polymer matrix at the level of individual tubes (Figure 1A). To the best of our knowledge, there are only few reported data for *solid* composites which display the same level of spectral resolution of the van Hove singularities.[34,35] PVA and PSS are expected to wrap SWNTs in the layers in the same way as they might do this in solution. In addition to the exfoliation of nanotubes into single strands, high-performance electrical composites require homogeneity of their distribution. This should translate into high probability of their intersection and, consequently, into the formation of an extensive network of conductive pathways. It is the interdigitation of the multilayers that leads to uniform distribution of the nanotubes in the matrix and formation of an extensive 3D network. This feature is a great advantage of LBL composites for charge transport because it increases the probability of formation of multiple contacts with other SWNTs and formation of an efficient charge-transfer pathway.

The state of high degree of debundling of the nanotubes in the films can also be confirmed by atomic force microscopy (AFM), scanning electron microscopy (SEM), and transmission electron microscopy (TEM) studies. The first layer indeed revealed a limited amount of SWNT adsorbed (Figure 2A) as expected from the ellipsometric measurements (Figure 1B). Apparent heights of the SWNT strands visible in Figure 2A are 1 to ∼3 nm, which matches well with the known information about SWNT diameters, mostly 1 to ∼2 nm[36] and occasionally reaching as low as 0.4 nm and as high as 4 nm.[1,37,38] Thicker (bright in AFM) spots in the midsections of some strands could be due to spontaneous accumulation of underlying polymers (both PVA and PSS) after adsorption (macromolecular crawling) rather than SWNT bundles previously observed in nanoparticle multilayers.[10] The exfoliation of SWNTs in an LBL film was corroborated by TEM images of $[PVA/(SWNT + PSS)]_2$ (Figure 3, parts A and B) and X-ray diffraction data (Figure S4, Supporting Information). The contrast of the TEM images is low because of the thinness of SWNTs which can be identified as long straight strands crossing the image in all directions. The low contrast of the images is informative in its own sense. It is indicative of the absence of SWNT bunching into much thicker aggregates and size separation of nanotube and polymer. The lack of the peak corresponding to SWNT bundles in small-angle X-ray scattering (SAXS) and wide-angle X-ray scattering (WAXS) spectra (Figure S4, Supporting Information) agrees well with the minimal degree of nanotube bundling in the films.

The surface roughness of LBL films measured from AFM and SEM images was ∼2.2 nm (Figure 2, parts A and B), which is similar to the ellipsometric thickness of an individual SWNT + PSS multilayer. One can also contemplate that each PVA sublayer is infiltrating the initial nanoscale nooks and crevices that random absorption of

(31) Dalton, A. B.; Collins, S.; Munoz, E.; Razal, J. M.; Ebron, V. H.; Ferraris, J. P.; Coleman, J. N.; Kim, B. G.; Baughman, R. H. *Nature* **2003**, *423* (6941), 703.
(32) Vigolo, B.; Penicaud, A.; Coulon, C.; Sauder, C.; Pailler, R.; Journet, C.; Bernier, P.; Poulin, P. *Science* **2000**, *290* (5495), 1331−1334.
(33) Zhang, M.; Atkinson, K. R.; Baughman, R. H. *Science* **2004**, *306* (5700), 1358−1361.
(34) Zhang, X.; Liu, T.; Sreekumar, T. V.; Kumar, S.; Moore, V. C.; Hauge, R. H.; Smalley, R. E. *Nano Lett.* **2003**, *3* (9), 1285−1288.
(35) Delozier, D. M.; Watson, K. A.; Smith, J. G.; Connell, J. W. *Compos. Sci. Technol.* **2005**, *65* (5), 749−755.
(36) Saito, R.; Dresselhaus, G.; Dresselhaus, M. S. *Physical Properties of Carbon Nanotubes*; Imperial College Press: 1998.
(37) Dresselhaus, M. S.; Dresselhaus, G.; Jorio, A. *Annu. Rev. Mater. Res.* **2004**, *34*, 247−278.
(38) Elliott, J. A.; Sandler, J. K. W.; Windle, A. H.; Young, R. J.; Shaffer, M. S. P. *Phys. Rev. Lett.* **2004**, *93* (14), 149602-1.

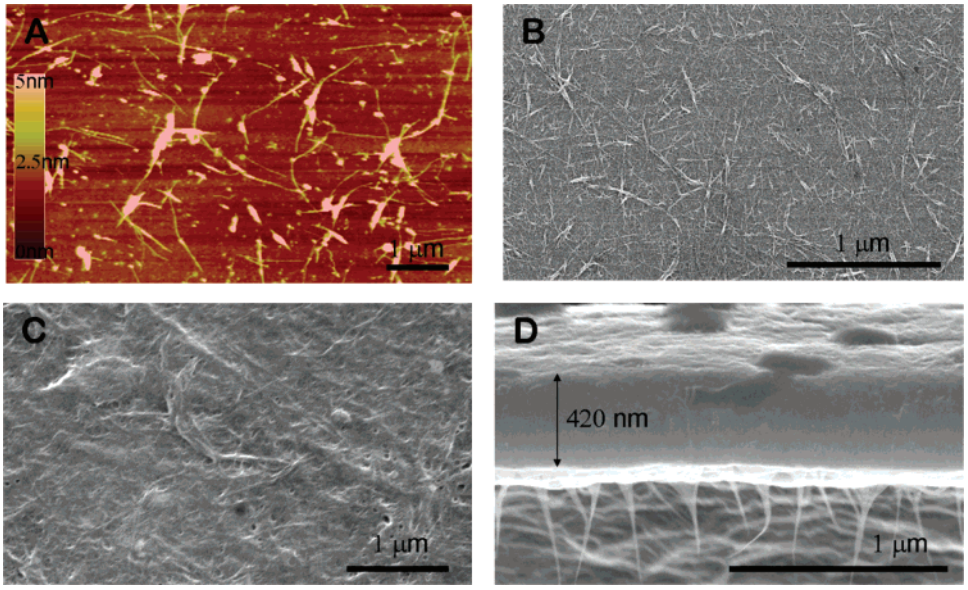

Figure 2. (A) AFM image of $[PVA/(SWNT + PSS)]_1$ and (B−D) SEM images of $[PVA/(SWNT + PSS)]_3$ (top view, B), $[PVA/(SWNT + PSS)]_{200}$ (top view, C), and $[PVA/(SWNT + PSS)]_{200}$ (cross section, D).

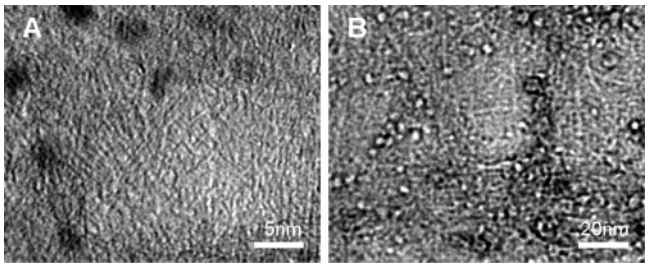

Figure 3. (A and B) TEM images of $[PVA/(SWNT + PSS)]_2$ over a thin PVA film.

SWNTs creates. We previously saw a similar process for LBL multilayers made from carbon fibers, which have much bigger diameter, i.e., 50−100 nm.[39] When crevices are filled, SWNTs are not only well-dispersed but also well-packed in the composite, which can be observed in a cross-sectional image of a 200-layer free-standing film, $[PVA/(SWNT + PSS)]_{200}$ (Figure 2D). The thickness of the LBL film was found to be 420 nm, which gives an average of 2.1 nm film increment per bilayer. This corresponds very well with the average thickness increment of 2.24 nm calculated from the ellipsometry measurements (Figure 1B).

Substantial accumulation of polymers between the SWNT strands can also be inferred from thermogravimetric analysis (TGA) used to estimate the nanotube contents of polymer composites. However, the TGA data often display the overlap of decomposition curves characteristic for several components. In the case of LBL assembly, one also needs to remember that the multilayer structure of the LBL composites where the inorganic phase sandwiches the polymers can significantly modify (increase) their characteristic decomposition temperature. To combat the overlap and related experimental errors, we analyzed TGA curves obtained in N_2 gas and in air environments. The gap between the data in N_2 and in air was plotted. After that, one can clearly observe the characteristic peaks of each component; PVA

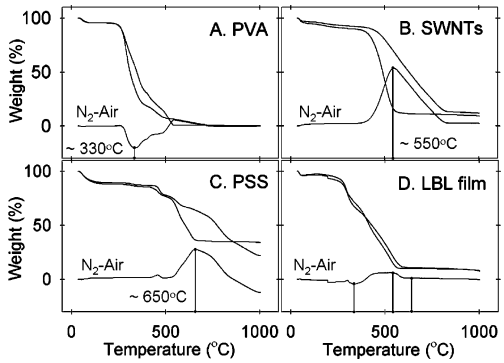

Figure 4. Thermogravimetric analysis of (A) PVA, (B) SWNTs, (C) PSS, and (D) $[PVA/(SWNT + PSS)]_{200}$ LBL film. Each sample was analyzed both in N_2 gas and air environment. The N_2–air curve at the bottom indicates the N_2–air residual gap which contains the LBL components' characteristic peaks.

330 °C, SWNT ∼550 °C, and PSS ∼650 °C (Figure 4A−C). These component peaks are also shown in the N_2–air residual gap analysis of the LBL film (Figure 4D). One can calculate the weight fraction of SWNTs as ∼10% of the peaks by comparing the ratio of SWNT peaks in N_2–air residual gap curves. This analysis is a more robust and reproducible tool for estimating the SWNT weight loading ratio in LBL films than classical TGA curves. Knowing the densities of PVA and SWNTs, i.e., 1.27 to ∼1.31[40] and 1.11 to ∼1.3,[41] respectively, the volume fraction of SWNTs can be determined as ∼10%. Although higher loadings of SWNTs might be beneficial, at least in some cases, for conductance in the composites, structural optimization of the SWNT−polymer system including preservation of its electronic structure has actually a much greater effect than the mass contents.

Electrical Conductivity of $[PVA/(SWNT + PSS)]_n$ LBL Films. Electrical conductivities in a SWNT−polymer com-

(39) Shim, B. S.; Starkovich, J.; Kotov, N. *Compos. Sci. Technol.* **2006**, *66* (9), 1174−1181.

(40) Lewis, R. J., Sr. *Hawley's Condensed Chemical Dictionary*, 14th ed.; John Wiley & Sons: 2002.

(41) Arnold, M. S.; Stupp, S. I.; Hersam, M. C. *Nano Lett.* **2005**, *5* (4), 713−718.

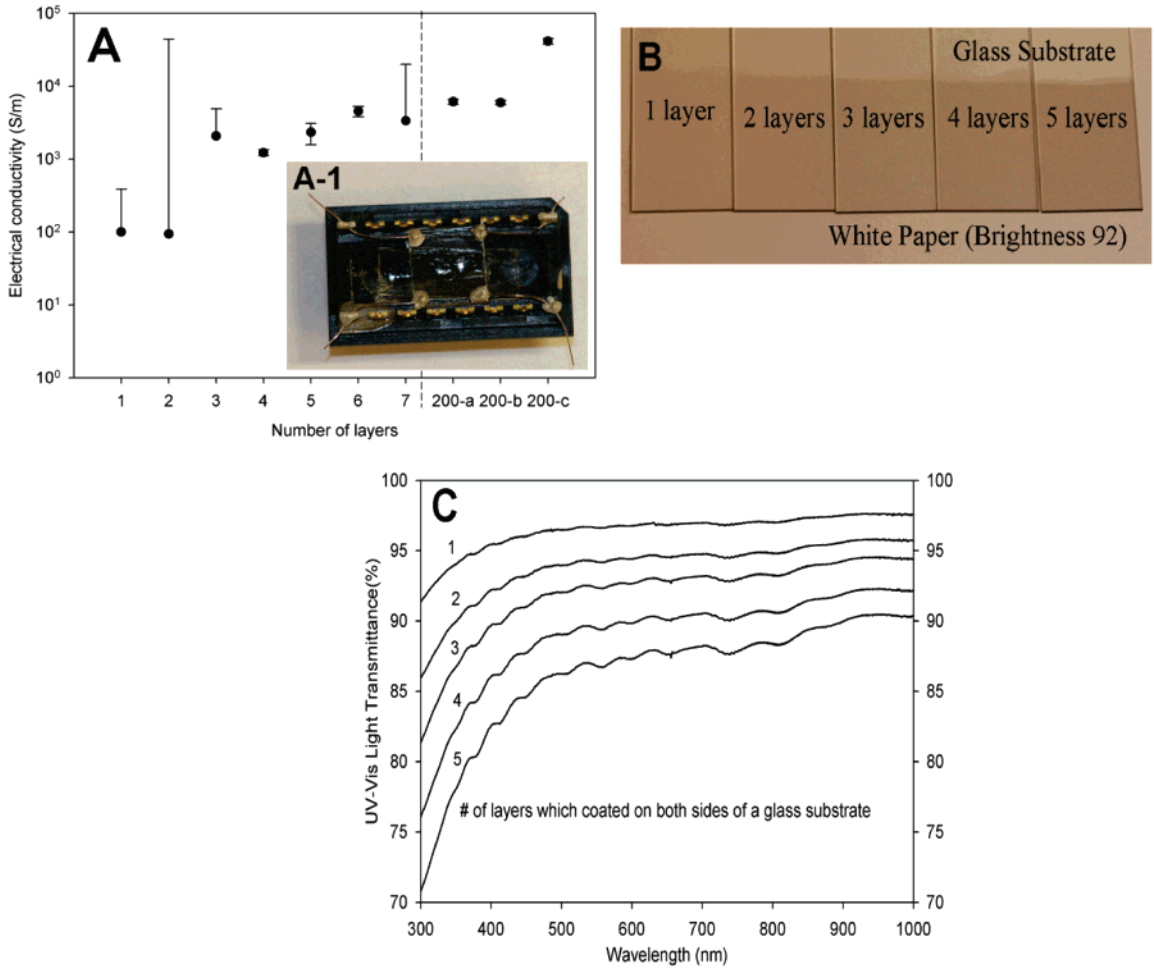

Figure 5. (A) Electrical conductivity measurements of $[PVA/SWNT + PSS]_n$ ($n = 1-7$, 200); 200-a, 200-b, and 200-c indicate as-prepared, 200 °C, and 300 °C treated films of 200 bilayers; LBL films with the van der Pauw measurement setup are shown in the inset. (B) Photograph and (C) UV−vis light transmittance of $[PVA/SWNT + PSS]_n$ ($n = 1-5$) LBL coatings on both sides of a glass substrate.

posite are based on charge percolation, which is the spontaneous formation of electrically conductive routes through an insulating matrix by a randomly distributed conducting filler. Normally, there is a dramatic conductivity change at the percolation threshold concentration of the filler. In addition, if the density of intersecting pathways above the percolation threshold is increasing, which happens when both the homogeneity and the volumetric ratio of SWNT distribution in the matrix are improved, then electrical conductivities still increase significantly.[28,42,43] As a matter of fact, the same effect can be achieved by increasing the specific spot attraction of SWNTs, i.e., by realization of the so-called "sticky contacts",[27] which might be achieved by biological conjugation,[44] but this property has to be carefully balanced with maintaining the uniform distribution of SWNTs.

Electrical measurements were carried out by the van der Pauw method assuming two-dimensionally isotropic conductivities and by the formation of electrical contacts between the sample and silver wires with conductive silver pastes (Figure 5A inset). For $[PVA/(SWNT + PSS)]_n$ LBL assemblies, the thicknesses of thin ($n = 1-7$) and thick ($n = 200$) films were estimated by ellipsometry (Figure 1B) and direct measurements of cross-sectional thickness (Figure 2D). Even the very thin layered films ($n = 1-2$) clearly indicated the conductivities much above the percolation threshold, 10^2 S/m. As more LBL layers were added ($n = 3-7$, 200), the conductivities increase to 2 to $\sim 5 \times 10^3$ S/m (with some samples readings as high as 3×10^4 S/m) (Figure 4A). A reasonable explanation to the gradual increase of the overall conductivity as the number of LBL layers increases is that SWNTs are adsorbed predominantly parallel to the substrate. The molecularly parallel layered adsorptions are intrinsic features of LBL assemblies, and high aspect ratio SWNTs naturally lie down on the surface rather than stand up. Thus, SWNTs in the film have two-dimensionally aligned structures even in a thick LBL film. The initial adsorption trends of SWNTs in Figures 1 and 2 are easily observed.

The controllability of the thickness with an increment of 2−3 nm implies precise tuning of the light transmission, which is important for a variety of optoelectronic devices as a replacement of ITO coating necessary to combat the shortage of indium. Light transmittance as high as 97% at 600 nm can be achieved for 5 nm films with conductivity in the range of 10^2 S/m (Figure 3, parts B and C) made after

(42) Shaffer, M. S. P.; Windle, A. H. *Adv. Mater.* **1999**, *11* (11), 937−941.
(43) Yang, Y.; Gupta, M. C.; Dudley, K. L.; Lawrence, R. W. *Nanotechnology* **2004**, *15* (11), 1545−1548.
(44) Lee, J.; Govorov, A. O.; Kotov, N. A. *Nano Lett.* **2005**, *5* (10), 2063−2069.

one deposition cycle. Notably, the actual transparency of single SWNT LBL coatings is even better than 97% because the light transmittance measurements in Figure 4, parts B and C, were performed with the samples in which both sides are coated on a glass substrate, not a single-side coating, whereas the conductivity is measured only on one side at a time.

One can obtain above 90% transmittance in the range of 400 to ~750 nm and conductivities of 10^2 to $\sim 2 \times 10^3$ S/m. Even though SWNT thin film made by filtering techniques may have a maximum conductivity of 10^5 to $\sim 10^6$ S/m with moderate transparency, their electrical percolation routes deteriorate above 90% of light transmittance.[22,45−48] For that reason only extrapolations based on empirical data at lower transparencies are typically provided for these films rather than the actual measurements.[22,45−48] When one looks at the combined structural, optical, and electrical data in conjunction with each other, it can be concluded that the utilization of SWNTs in LBL films is exceptionally efficient due to high homogeneity and degree of dispersion of the nanotubes in them (Figure 1). Another noticeable distinction from SWNT mats is that LBL films can be directly coated on a variety of complex surfaces. Examples when this property may become very essential include optical fiber, microfluidic channels, and the porous surfaces of flexible moving structures.

LBL assemblies of SWNT−PVA can be expanded to fabricate a membrane-like flexible free-standing film detached from the substrates. The electrical conductivity of the as-prepared 200-layered film measured by the same van der Pauw technique was 6.1×10^3 S/m. Thermal treatment of the film at 200 °C makes little change in the conductivity, while increase of the annealing temperature to 300 °C boosts it further to 4.15×10^4 S/m. After the creation of the percolation network, the improvement of the quality of SWNT−SWNT contacts is one of the most important requirements to the design of electrically conductive SWNT composites, because the efficiency of electron tunneling through the gap is exponentially dependent on the SWNT−SWNT distance. So, the effect of heat treatments can be understood as a gradual closing of intrinsic nano- and angstrom-scale voids/pores and relaxation of the polymer conformation to the one that adheres to nanotubes better. Altogether, this makes better contact between individual SWNTs in the network. The temperature threshold of conductivity improvement, i.e., 200−300 °C, corresponds very well with the expected melting temperature of PVA in the LBL films. Although heat treatment effects onto nanostructures of our SWNT LBL composite were not simple, thickness changes of the film were 5% and 10% reduction with 200 °C and 300 °C treatments. A more detailed and formal description of temperature effect is given in the Supporting Information.

Mechanical Properties of Conductive LBL Films. The strength of the transparent thin films is also an important parameter when it comes to device manufacturing. Although the strength of very thin films cannot be directly quantified, the integrity of the films was not affected at all when we rubbed the surface and cut it into a small square (4 mm × 4 mm) to fit our van der Pauw measurement setups. To quantify these empirical observations, mechanical properties of fairly thick $[PVA/SWNT + PSS]_{200}$ films were measured. The mechanical strength of the thick LBL film was estimated before and after 200 °C heat treatment by direct sample stretching tests (ASTM D 3039). Tensile strengths/strains of the sample were 150 ± 18 MPa/6% before and 159 ± 21 MPa/5% after the heat treatment, respectively (Figure 6, parts A and B). It makes the LBL films around 2 to ~10 times stronger than the bucky papers.[20,49] They are also exceptionally flexible (Figure 6, parts C and D), which cannot be attributed to SWNT mats without the polymer impregnation.

Phenomenological Analysis of Conductivity in LBL Films. One of the advantages of LBL films is that one can engineer their nanoscale and molecular structure to obtain desirable properties. In this respect, we need to map out potential directions for further improvement of their electrical characteristics. In order to do that let us consider the linear reversible electrical conductivity decrease with temperature increase in the set composite leading to more fundamental understanding of electrical transport in LBL structures. It can be explained by taking into account (1) semiconducting characteristics of SWNTs and (2) Schottky barriers or structural mismatch in metallic and semiconducting SWNT junctions.[29,50] The electrical resistance ($R_{composite}$) of a SWNT−polymer composite is associated with intrinsic semiconducting or metallic SWNT resistances (R_{SWNTs}) and SWNT−SWNT contact resistances ($R_{contact}$) between the nanotubes because the polymer matrix in this system is an electrical insulator.[51] Despite significant improvement of electrical parameters, the electrical conductivities of a composite are below the axial direction measured conductivities of individual SWNTs, 1 to $\sim 3 \times 10^6$ S/m.[3] This leads to the conclusion that the SWNT−SWNT contact resistances in a composite dominate the total resistance of a composite ($R_{contact} \gg R_{SWNTs}$). The SWNT−SWNT contact resistance ($R_{contact}$) is further factored into SWNT junction resistances including semiconducting−semiconducting (R_{SS}), semiconducting−metallic (R_{SM}), and metallic−metallic (R_{MM}) which are much different in their magnitude ($R_{SM} \gg R_{SS} > R_{MM}$).[29] However, SWNT junctions in a well-dispersed SWNT−polymer composite are not simply formed as physically perfect contacts. Instead, very thin polymeric layers, which are essential in an LBL system, are often likely to be sandwiched between the tubes preventing the pure ohmic contact. Note that the polymer is a necessary part of the SWNT-based material which allows one to make macro-

(45) Wu, Z.; Chen, Z.; Du, X.; Logan, J. M.; Sippel, J.; Nikolou, M.; Kamaras, K.; Reynolds, J. R.; Tanner, D. B.; Hebard, A. F.; Rinzler, A. G. *Science* **2004**, *305* (5688), 1273−1277.
(46) Hu, L.; Hecht, D. S.; Gruener, G. *Nano Lett.* **2004**, *4* (12), 2513−2517.
(47) Zhou, Y.; Hu, L.; Gruner, G. *Appl. Phys. Lett.* **2006**, *88* (12), 123109-1−123109/3.
(48) Gruner, G. *J. Mater. Chem.* **2006**, *16* (35), 3533−3539.
(49) Sreekumar, T. V.; Liu, T.; Kumar, S.; Ericson, L. M.; Hauge, R. H.; Smalley, R. E. *Chem. Mater.* **2003**, *15* (1), 175−178.
(50) Avouris, P. *Acc. Chem. Res.* **2002**, *35* (12), 1026−1034.
(51) Bae, D. J.; Kim, K. S.; Park, Y. S.; Suh, E. K.; An, K. H.; Moon, J. M.; Lim, S. C.; Park, S. H.; Jeong, Y. H.; Lee, Y. H. *Phys. Rev. B: Condens. Matter Mater. Phys.* **2001**, *64* (23), 233401-1−233401/4.

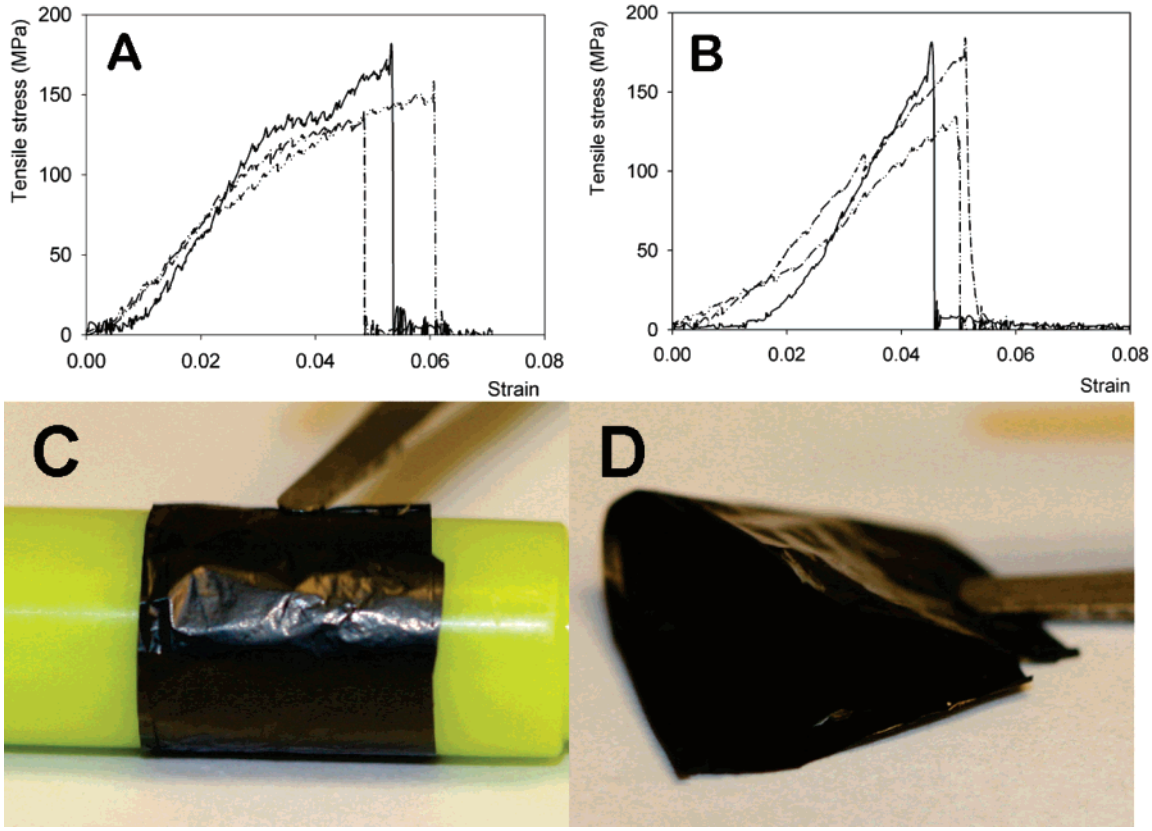

Figure 6. Mechanical stretching test results of the $[PVA/(SWNT + PSS)]_{200}$ LBL film (A) before and (B) after 200 °C heat treatment. (C and D) Demonstration of the flexibility of an LBL composite film which is contrasted with brittle SWNT-only mats.

scopic objects. Since the polymers used here are insulating, one can safely assume that $R_{polymer} \gg R_{SM}$. Therefore, $R_{contact}$ can be substituted with one of R_{SS}, R_{SM}, R_{MM}, and $R_{polymer}$. Taking a single electrical conductive route, one can represent it as a series of SWNT−SWNT contacts, whose electrical resistance is simply a sum of all these resistances.

$$R_1 = x[R_{SWNTs} + R_{contact}] = xR_{SWNTs} + x_1R_{SS} + x_2R_{MS} + x_3R_{MM} + x_4R_{polymer} \quad (1)$$

where $x = x_1 + x_2 + x_3 + x_4$.

If a composite has anisotropic molecular structures such as SWNT alignment, the magnitude of x significantly decreases. Numerous electrically conductive routes exist which are considered as parallel circuits in a SWNT−polymer composite. Therefore, the reciprocal of total resistance ($1/R_{tot}$), conductance (G_{tot}), of a composite can be calculated as a sum of the reciprocals of electrical resistances from possible conductive routes.

$$1/R_{tot} = 1/R_1 + 1/R_2 + ... + 1/R_y = G_{tot} \quad (2)$$

From this analysis, we can set the priority of the optimization process for improving electrical conductivity because the largest resistance term dominates the total resistance of a composite. The first stage of the optimization is to minimize the term, $x_4R_{polymer}$, which was achieved here by thermal treatment tightening (see the Supporting Information, Figure S1), because it apparently reduced the gap between the nanotubes (Supporting Information Figure S2). The second stage should be modification of R_{SM} to R_{SS} or R_{MM} because R_{SM} is much larger than R_{SS} or R_{MM} and x_1, x_2, and x_3 are all the same order of magnitude. However, current technology can produce only SWNT mixtures so that the semiconducting−metallic Schottky junctions will remain the main contributors to the remaining electrical resistance until the SWNT separation problem is solved. At last, the third stage is to minimize the magnitude of x, the number of SWNT contacts, and more specifically, hopping probability of a charge carrier. Creating anisotropic nanoscale structures such as SWNTs layered structures or alignments or using longer conducting fillers could be options to reduce x. In the other respect, bundling of SWNTs may dramatically limit the number of percolation routes, the magnitude of y, number of effective conductive routes, although SWNT ropes may generate reduced x and, sometimes, the composite to be metallic. The reduction of effective conductive routes is a critical issue because of structural mismatch of SWNTs which implies that not every SWNT junction is effective site for charge carrier hopping.[50] Therefore, exfoliation in single-stranded SWNT indeed increases the electrical conductivities by increasing the total numbers of conductive routes with the same SWNT filling ratio.

Using the language of this analysis, one can say that the heat treatment improves the quality of SWNT−SWNT contacts by partially removing polymer sandwiched between them. SWNT LBL composites have much bigger y than bucky paper because bundled SWNTs of a bucky paper critically decrease the possible number of conductive routes, y. Hence, SWNT LBL composite with an order of magnitude lower SWNT contents could demonstrate the level of

electrical conductivities not too far from some SWNT-only bucky papers.

Conclusion

In this article, we described electrical properties of pristine SWNT−polymer LBL film and demonstrated effective reinforcement, unique optical transparencies, and useful electrical conductivities with small SWNT contents. The described SWNT−polymer LBL composites created effective SWNT−SWNT contacts due to a high degree of exfoliation, high homogeneity, and a thermal tightening of gaps between them. The electrical conductivities measured in the LBL films were substantially higher than most of other PVA−SWNT or polymer−SWNT composites which have conductivities of 10^{-2} to 10^{4} S/m.[42,52,53] In comparison to conductivities of SWNT mats made of pure nanotubes[18,20,45,49,54−58] (10^{4} to $\sim 10^{6}$ S/m), the conductivities here are lower. Although not exceeding the 10^{6} S/m record, the LBL films fill the functional property gap between pure SWNT films and SWNT−polymer composite system. We should make three points about the LBL structures: (1) the SWNT loading is more than an order of magnitude smaller than in other thin films, (2) the SWNTs were not doped, and (3) polymers we used are insulators. The conductivities of the composite can potentially be improved several orders of magnitude by addressing these aspects in the future structures. The current electrical and mechanical data demonstrate of effective transfer of SWNT properties in organic thin films, which could be applied in numerous fields, from solution-processed transparent flexible organic electronics and light harvesting to physicochemical sensors in biomedical, space, and civil engineering.

(52) Grossiord, N.; Loos, J.; Regev, O.; Koning, C. E. *Chem. Mater.* **2006**, *18* (5), 1089−1099.
(53) Guo, H.; Sreekumar, T. V.; Liu, T.; Minus, M.; Kumar, S. *Polymer* **2005**, *46* (9), 3001−3005.
(54) Bekyarova, E.; Itkis, M. E.; Cabrera, N.; Zhao, B.; Yu, A.; Gao, J.; Haddon, R. C. *J. Am. Chem. Soc.* **2005**, *127* (16), 5990−5995.
(55) Fischer, J. E.; Dai, H.; Thess, A.; Lee, R.; Hanjani, N. M.; Dehaas, D. L.; Smalley, R. E. *Phys. Rev. B: Condens. Matter* **1997**, *55* (8), R4921−R4924.
(56) Kim, G. T.; Choi, E. S.; Kim, D. C.; Suh, D. S.; Park, Y. W.; Liu, K.; Duesberg, G.; Roth, S. *Phys. Rev. B: Condens. Matter Mater. Phys.* **1998**, *58* (24), 16064−16069.
(57) Kaiser, A. B.; Dusberg, G.; Roth, S. *Phys. Rev. B: Condens. Matter Mater. Phys.* **1998**, *57* (3), 1418−1421.
(58) Bozhko, A. D.; Sklovsky, D. E.; Nalimova, V. A.; Rinzler, A. G.; Smalley, R. E.; Fischer, J. E. *Appl. Phys. A: Mater. Sci. Process.* **1998**, *A67* (1), 75−77.

Experimental Section

Materials. Poly(vinyl alcohol) (PVA; MW, 70 000 to ~100 000) and poly(sodium 4-styrene-sulfonate), (PSS; MW, 1 000 000) were purchased from Sigma-Aldrich Co. The purified HiPco SWNTs used for the experiment were purchased from Carbon Nanotechnologies Incorporated (CNI).

LBL Assembly. Purified HiPco SWNTs were dispersed in 0.2 wt % PSS solution with 2 days of mild sonication in a VWR model 150HT ultrasonic cleaner.[23] The dispersion with 1 mg/mL of SWNTs was centrifuged at 5000 rpm, and then the supernatant was collected, which became one LBL component. PVA solution (1 wt %) was prepared for another LBL partner. Detailed procedures of LBL assemblies between SWNTs and polymer are described in the previous publication from our group.[8] By charge-transfer interaction between PSS which are wrapping SWNTs and PVA, or by hydrogen bonding between possible COOH groups in SWNTs and OH in PVA, they formed LBL assemblies on a charged substrate (glass or Si). Each LBL layering process consists of 10 min of dipping in the PVA or in the SWNT solution, rinsing in deionized water, and drying. To denote LBL assemblies, $[\text{PVA/SWNT} + \text{PSS}]_n$ was used in which n represents the number of repeated dipping processes in PVA and SWNT solutions.

Instrumental Analysis. Scanning electron microscopy images were taken with a Philips XL30 field emission gun scanning electron microscope and an FEI Nova Nanolab dual-beam FIB and scanning electron microscope. Atomic force microscopy imaging was performed with a Nanoscope III (Digital Instruments/Veeco Metrology Group). UV−vis absorption measurements were taken using an Agilent 8453E UV−vis spectrophotometer. An Agilent 34401A multimeter was used for electrical measurements. Mechanical tests were done by a Q systems model 100 (Test Resources). Thermogravimetric analysis was performed by a Perkin-Elmer Pyris 1 TGA. Ellipsometric measurements were done by an M-44 IR spectroscopic ellipsometer (J. A. Woollam Co., Inc.).

Acknowledgment. N.A.K. thanks the AFOSR, ONR, and NSF for the support of this research.

Supporting Information Available: SWNT tightening by thermal annealing, and SWNT concentration effects of LBL films (PDF). This material is available free of charge via the Internet at http://pubs.acs.org.

CM070442A